

# Online Monitoring of Bromate in Ozonized Water Without a Previous Separation Process

M. J. Almendral-Parra · A. Alonso-Mateos ·  
M. S. Fuentes-Prieto

Received: 18 February 2008 / Accepted: 14 March 2008 / Published online: 24 July 2008  
© Springer Science + Business Media, LLC 2008

**Abstract** The use of ozonation for the purification of drinking water can lead to the formation of bromate. The US Environmental Protection Agency and the European Directive for human drinking water has lowered the regulatory level for bromate down to  $10 \mu\text{g l}^{-1}$ , such that methods must be developed for monitoring the formation of bromate, particularly in on-site situations. In the present work we report a fluorometric method for the determination of bromate based on the reaction with carbostyryl-124, a compound that shows fluorescence mainly at pH values above 4 and, when bromated, generates a non-fluorescent product. The reaction can thus be used as an indirect method for determination of the ion. The proposed method, which uses the flow injection (FI) technique, allows online application and kinetic control of the variables affecting the process, together with shorter reaction times, and it provides maximum sensitivity and selectivity. Under optimum conditions, it is possible to determine the analyte within the  $4\text{--}200 \mu\text{g l}^{-1}$  range, with a limit of detection of  $0.9 \mu\text{g l}^{-1}$  and a relative standard deviation ( $n=12$ ,  $[\text{BrO}_3^-]=5$  and  $30 \mu\text{g l}^{-1}$ ) of 3.2% and 2.6% respectively. The determination rate was ten samples per hour.

**Keywords** Bromate · Water · Fluorimetry · Flow injection analysis · Carbostyryl-124 · Disinfection by-product

## Introduction

Water destined for human consumption must be subjected to a series of treatments aimed at eliminating pathogenic agents and reducing other pollutants to acceptable levels that are not harmful to health. In this process, chemical treatment—and within this disinfection—is important. The disinfection process involves different physical, biological and chemical treatments. The latter can be performed with chlorinated products (chlorine, chloramines, chlorine dioxide), ozone, potassium permanganate, quaternary ammonium salts, etc. In its different forms, chlorine is the chemical agent most widely used. Although the attention of many researchers has focused on the by-products of chlorine disinfection, other chemical disinfecting agents also generate by-products when they react with organic substances and other precursors present in untreated water. Bromate, for instance, is essentially a by-product of the ozonation of water with high bromide contents [1, 2] and amounts between  $60\text{--}90 \mu\text{g l}^{-1}$  have been found in ozonized water.

Chronic exposure to  $\text{KBrO}_3$  causes kidney cell tumors in rats, hamsters and mice, and thyroid and testicular mesothelial tumors in rats [3–5]. Owing to its cross-species carcinogenicity, bromate is considered a probable human carcinogen by the International Agency for Research on Cancer (IARC) [6]. It also has a potential negative effect on health, which can damage the nervous system, kidney and thyroid gland [7]. European Directive 98/83 /CEE of 3 November 1998 on the quality of water intended for human consumption establishes that the maximum contaminant level (MCL) of bromate in drinking water should be  $10 \mu\text{g l}^{-1}$  [8] as from 2009, accepting values of up to  $25 \mu\text{g l}^{-1}$  for the period between 2004 and 2008. This gives countries the chance to achieve lower values, when possible, without this affecting disinfection quality. This guideline value is

M. J. Almendral-Parra (✉) · A. Alonso-Mateos ·  
M. S. Fuentes-Prieto  
Departamento de Química Analítica, Nutrición y Bromatología,  
Faculty of Chemistry, University of Salamanca,  
Plaza de la Merced s/n,  
37008 Salamanca, Spain  
e-mail: almendral@usal.es

provisional because of limitations in available analytical and treatment methods, and there is an urgent need to set up techniques able to detect levels of  $2.5 \mu\text{g l}^{-1}$  or even lower. The US Environmental Protection Agency (US EPA) has proposed to set the maximum contaminant level for bromate ion in drinking water at  $10 \mu\text{g l}^{-1}$  [9]. In order to control this value in real samples, fast automated analysis systems are required.

The literature contains many references to methods for the analysis of bromate in matrices with concentrations ranging from  $\mu\text{g l}^{-1}$  to  $\text{mg l}^{-1}$ . According to the US EPA., during the nineties, the maximum pollutant level expected lay between 0.1 and  $1 \text{ mg l}^{-1}$ . The first methods were developed to meet this objective but since the limit value of bromate was reduced to  $10 \mu\text{g l}^{-1}$  during the past decade the development of new methods has focused on improving sensitivity [10].

Ion chromatography (IC) with conductivity detection (IC-CD) is the technique most widely employed. The determination of bromate by means of this technique has a limit of detection of  $20 \mu\text{g l}^{-1}$  (method 300.0, 1989 of the EPA [11]). Using a chromatographic system with preconcentration, it is possible to attain a limit of detection of  $1.3 \mu\text{g l}^{-1}$ . This, however, has the drawback of being subject to the action of many interferents (such as chloride) and requires steps prior to sample introduction into the instrumental system, which prolongs analysis times. The method must be improved as regards the identification and pretreatment of samples. Recently, a new ion exchange column has been developed that seems to overcome the problems of interference and does not require a preconcentration step. The sensitivity of the technique has been increased in two ways: improving the technology of the columns (lowering the detection limit to  $1.3 \mu\text{g l}^{-1}$  (method 300.1, 1997, [12]) and performing sample pretreatment to remove the main interferents (standard ISO 15061 method [13]), attaining a limit of detection of  $0.5 \mu\text{g l}^{-1}$ . The method has been modified by post-column reaction with KBr-*o*-dianisidine reagents [14], and the removal of  $\text{ClO}_2$  with Fe(II) (EPA Method 317.0) [15]. A bromate-specific method (EPA Method 324.0) [16] and post-column reaction methods (EPA Method 326.0) [17, 18] have also been proposed.

Inductively coupled plasma-mass spectrometry (ICP-MS) can be coupled with IC [19–21] or flow injection systems [22], affording a detection limit of  $0.1\text{--}0.3 \mu\text{g l}^{-1}$  of bromate, which can be further reduced to  $0.05 \mu\text{g l}^{-1}$ . Moreover, some analytical methods based on spectrophotometric detection after post-column reaction [14, 23, 24], gas chromatography [25], chemiluminescence detection [26] and electrospray IC-tandem mass spectrometry [27, 28] have also been reported for the determination of bromate [29].

Few fluorimetric methods have been reported for the determination of bromate, among them ion chromatography with a fluorescence detector using the post-column reaction of the bromation of carbostyryl-124 (CARB) in acid medium. This method has two pitfalls: the need to use a very long reactor, thus extending the analysis time, and an important degree of interferences from the  $\text{ClO}_2^-$  ion. The quantification rate is  $1.6 \mu\text{g l}^{-1}$  [10].

Although these techniques meet the requirements of current legislation, they are relatively complex, time consuming and require high-technology and expensive instrumentation; they are thus not suited for routine on-site monitoring. In order to monitor ozonation and to control bromate in drinking water on-site, simple, low-cost and robust methods are necessary.

Among the non-chromatographic methods, spectrofluorimetry is a sensitive technique that can be readily adapted for online determinations. Here we report a fluorimetric procedure for bromate determination based on the above carbostyryl reaction, with no a previous separation process, using flow injection analysis (online application) and kinetic control of the variables affecting the reaction, achieving shorter reactions times with maximum sensitivity and selectivity.

## Experimental

### Apparatus and materials

Minipuls HP4 (Gilson, France) peristaltic pumps with silicone or vinyl pump tubes. PTFE simple-injection valve (Rheodyne, model 5020). Detection was performed with an RF-5000 spectrofluorimeter (Shimadzu, Japan) fitted with a DR-15 data processor and an FDU-13 data storage unit, to which a sensitization unit was coupled, (Shimadzu, 200-26841-01). A 25- $\mu\text{l}$  flow cell (Hellma, Germany, 176.052) with an optical pathway of 0.150 cm and a rectangular quartz flow cell (Shimadzu, 204-05566) of 1 cm optical pathway and 12  $\mu\text{l}$  volume were employed. PTFE tubing of 0.5 mm internal diameter with standard tube fittings and connectors (Upchurch Scientific, Inc.) was used. A Crison 501 potentiometer and a Digiterm 3000542 (Selecta) water bath thermostatted at  $27^\circ\text{C}$  were also used.

### Reagents and solutions

All chemicals used in this work were of analytical grade and were prepared with ultra-high quality deionized water.  $5.02 \times 10^{-4}$  M solution of carbostyryl-124 (CARB, Aldrich) prepared by weighing the reagent and dissolution in distilled water, to which 20.0 ml of 12 M HCl (Panreac) and 10 g of solid KBr (Carlo Erba) had been added.

Solution 1.26 M of sodium acetate (Prolabo). Standard concentrated solutions of  $1.0017 \text{ g l}^{-1}$  of potassium bromate,  $\text{KBrO}_3$ , (Panreac) and of  $0.4200 \text{ g l}^{-1}$  of sodium chlorite,  $\text{NaClO}_2$ , (Acros organics). Working standard solutions were prepared after suitable dilutions of the stock solution with distilled water. Solutions of a large number of inorganic ions prepared from their water-soluble salts were also used.

### Flow System

Figure 1a shows the flow scheme proposed for the determination of  $\text{BrO}_3^-$  by means of the CARB bromation reaction and fluorimetric measurement of the excess reagent after the reaction.

The device has three channels and two peristaltic pumps. Channel  $C_1$  carries the CARB reagent dissolved in HCl medium, at a strongly acid pH and in the presence of excess KBr. Channel  $C_2$  carries a constant flow of bidistilled  $\text{H}_2\text{O}$ , which acts as carrier, into which a volume of standard solution or sample containing  $\text{BrO}_3^-$  is injected. Both solutions merge at a confluence point (T connection) where the bromation reaction of the CARB reagent begins, this consisting of two steps: the reaction between  $\text{BrO}_3^-$  and  $\text{Br}^-$  to generate bromine and the bromation of the CARB reagent.

From the first point of confluence to the second one, the reaction time is controlled, together with the flow rates  $F_R$

and  $F_P$ , with a 0.5 mm inner diameter Teflon reactor of variable length. In order to control the reaction temperature, the reactor is placed in a thermostatted water bath. Channel  $C_3$  carries a continuous flow of a solution of NaAc, with a flow rate of  $F_A$ , at a suitable concentration, so that when channels  $C_1$  and  $C_2$  meet the resulting pH will be appropriate for the measurement of the fluorescence generated by the excess CARB from the bromation reaction ( $\lambda_{\text{exc}}=339 \text{ nm}$ ,  $\lambda_{\text{em}}=430 \text{ nm}$ ). The excitation and emission slit widths are maintained at 10 nm at all times. Throughout the study a flow cell of  $25 \mu\text{l}$  was employed; this was introduced into the fluorimeter in a sensitization unit for greater optical efficiency (with concave mirrors).

Once the chemical variables and the flow rate had been optimized, in order to study the rest of the geometric and hydrodynamic variables a practical modification of the flow scheme depicted in Fig. 1 was made (Fig. 1b). A peristaltic pump controlled the flow rate of the carrier solution,  $F_P$ , which was kept at a value of  $0.38 \text{ ml min}^{-1}$ , while with the second peristaltic pump  $F_R$  and  $F_A$  were controlled at the same time; these were kept at the same value of  $0.10 \text{ ml min}^{-1}$ . This new system allowed the flow rate at which the sample was injected to be independent of the flow rate of the reagents, allowing sample dilution to be controlled. Using this flow system, the analytical calibrations were performed, together with the study of interferences and validation of the method.

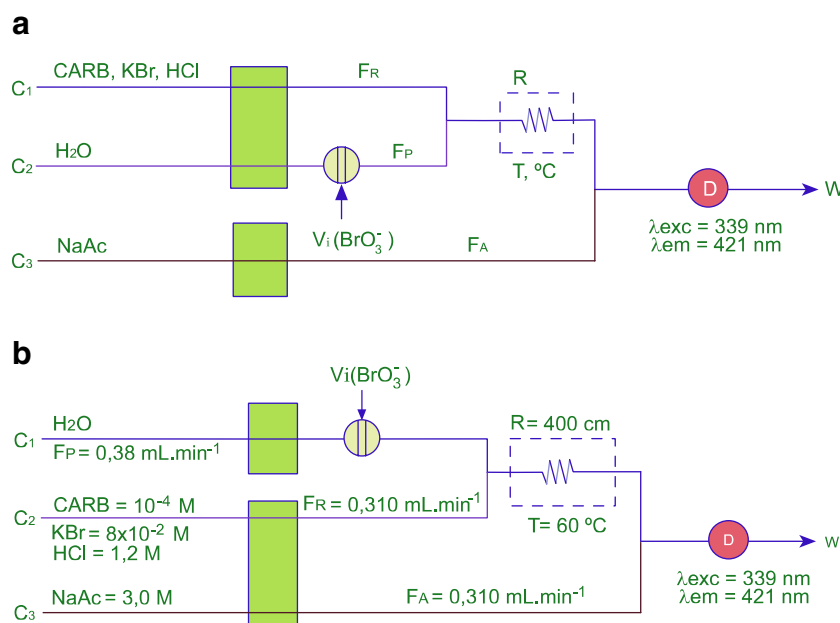


**Fig. 1** **a** Flow scheme proposed for the determination of  $\text{BrO}_3^-$  in continuous mode by means of the CARB bromation reaction. Fluorimetric determination of the excess reagent. CARB carbostyryl-124,  $F_R$ ,  $F_P$  and  $F_A$  flow rates of the solutions carried through  $C_1$ ,  $C_2$

and  $C_3$ ,  $V_i$  injection volume,  $R$  reactor,  $D$  fluorimeter. **b** Optimum flow scheme for the determination of  $\text{BrO}_3^-$  by means of the carbostyryl-124 bromation reaction

## Results and discussion

### Fluorescence spectra

The 7-amino-4-methyl-2-hydroxyquinoline:  $C_{10}H_{20}N_2O$  is commercialized under different names. One of them, used in the proposed method, is carbostyryl-124, a compound that is insoluble in HCl and that mainly shows fluorescence at pH values higher than 4 and that, upon bromation, generates a non-fluorescent product. This reaction is therefore used as an indirect method for the determination of  $BrO_3^-$  after separation by ion chromatography. The decrease in fluorescence is proportional to the concentration of  $BrO_3^-$ .

Figure 2 shows the excitation spectra of CARB at pH 4.8 at the optimum  $\lambda_{em}$  (430 nm) and the emission spectra, at the same pH value, obtained with the optimum  $\lambda_{ex}$  (339 nm). The same solution of CARB, but at more acid pH values, afforded the same spectra but with lower fluorescence intensities, fluorescence disappearing at pH values below 2. The protonated forms did not emit fluorescence. Above a pH of 4.3, the fluorescence remained constant, owing to the predominance of the basic form of the organic molecule.

When KBr and excess  $KBrO_3$  (excess bromation) were added to an acid solution containing CARB, adjusting pH to 4.8, the final solution did not show fluorescence because the bromation product formed was not fluorescent (bromation on carbons with double bonds).

When designing the flow scheme the pH conditions for the bromation reaction (a strongly acid medium) and the pH zone for the measurement of the fluorescence of the excess reagent, with a pH above 4.3, were taken into account.

The solutions of CARB in HCl medium were stable for at least 8 days after their preparation. This was checked by measuring fluorescence during that period of time and conserving them under refrigeration.

Figure 3 shows the analytical signal obtained upon injecting in duplicate a standard solution of  $BrO_3^-$  under suitable experimental conditions. The baseline corresponds to the emission of fluorescence by the CARB reagent at the pH of the second point of confluence ( $>4.3$ ). When a volume of a standard solution of  $BrO_3^-$  was injected, it reacted with the  $Br^-$  contained in the reagent solution at acid pH, generating  $Br_2$ , which reacted with CARB to form a non-fluorescent compound. The analytical signal generated was negative, since it measured the decrease in fluorescence intensity due to the decrease in the CARB concentration. The height of the diagram,  $\Delta I_F$ , was directly proportional to the concentration of the oxidant,  $BrO_3^-$ .

### Preliminary studies

#### *Kinetic characteristics of the reaction*

*Influence of reactor length* In light of the difficulty involved in performing a kinetic study of the reaction in discontinuous mode, owing to the problem of the difference in the optimum pH for the chemical reaction and for fluorescence emission, kinetic data concerning the chemical reaction were obtained by operating in continuous mode, since this is performed at a preset time with the possibility of controlling both pH values simultaneously.

In the flow scheme depicted in Fig. 1a the following conditions were imposed: Channel  $C_1$ :  $[CARB]=10^{-4}$  M,  $[KBr]=6.7 \times 10^{-2}$  M,  $[HCl]=0.8$  M,  $F_R=0.24$  ml  $min^{-1}$ ; Channel  $C_2$ : Water as carrier,  $V_i=243$   $\mu$ l of a standard solution of  $BrO_3^-$  at a concentration of 200  $\mu$ g  $l^{-1}$ ,  $F_P=0.24$  ml  $min^{-1}$ ; Channel  $C_3$ :  $[NaAc]=2.5$  M,  $F_A=0.24$  ml  $min^{-1}$ . Although these were not optimum conditions, it was possible to guarantee a sufficiently acid pH for the  $BrO_3^- - Br^-$  reaction to occur, and the high NaAc concentration ensured that the pH of the second confluence point was

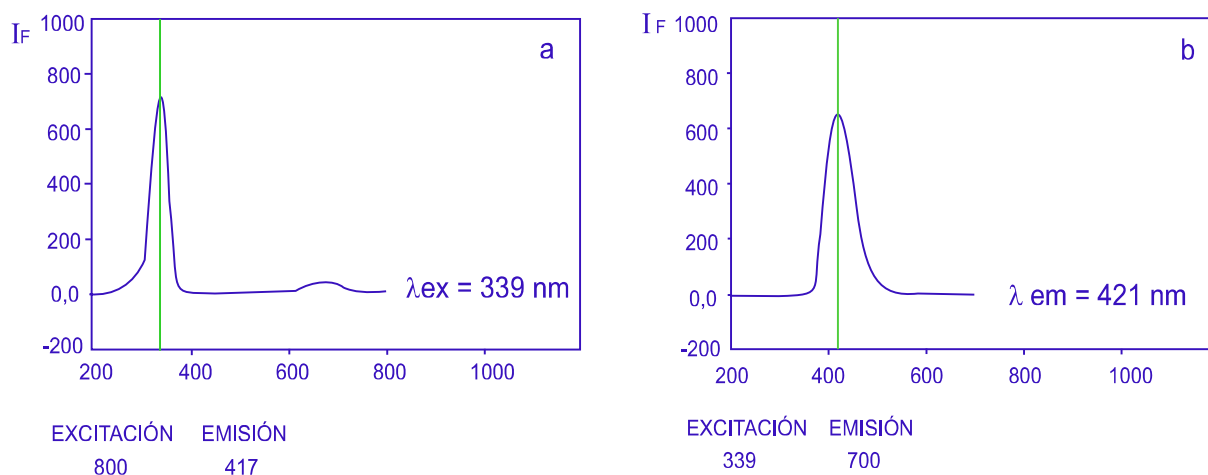


**Fig. 2** Spectra **a** excitation, **b** emission, of carbostyryl-124 at pH 4.8. Deduction of optimum  $\lambda_{exc}$  and  $\lambda_{em}$

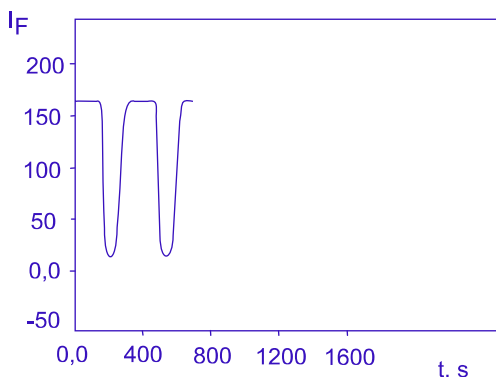


**Fig. 3** Typical diagrams obtained upon the injection of 243  $\mu\text{l}$  of a standard solution of bromate in duplicate ( $\lambda_{\text{exc}}=339\text{ nm}$ ;  $\lambda_{\text{em}}=421\text{ nm}$ )

higher than 4.3 in order to achieve maximum fluorescence emission. Under these conditions, the length of the reactor was changed from 300 to 1,350 cm at room temperature (23 °C).

The values of  $\Delta I_F$  are shown in Fig. 4 versus the reactor length (bottom) and reaction time (top). It may be seen that under these experimental conditions the reaction exhibits slow kinetics, the analytical signal increasing with the increase in the reaction time and tending to a constant value for times longer than 344 s. In no case, not even for very long reactors, did dispersion predominate over the increase in the analytical signal.

**Influence of temperature** With the same experimental conditions as those used before, the reactor length was fixed at 400 cm and the device was thermostatted at different temperatures between 23 and 80 °C. The reaction time was the same for all the experiments ( $t_R=110\text{ s}$ ) and the contact time between the reagent bolus and the

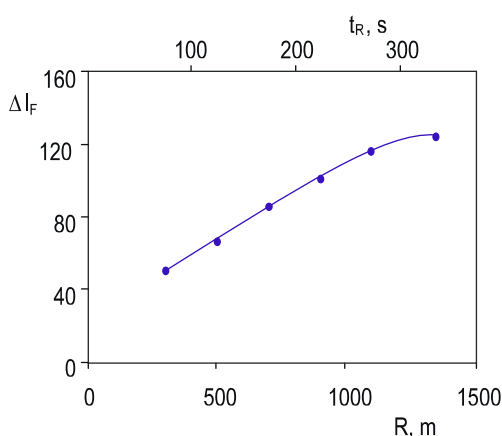


**Fig. 4** Determination of  $\text{BrO}_3^-$  in continuous flow mode by means of the bromation reaction of carbostyiril-124. Kinetic evolution of the reaction at room temperature.  $C_1$ :  $[\text{CARB}]=10^{-4}\text{ M}$ ,  $[\text{KBr}]=6.7 \times 10^{-2}\text{ M}$ ,  $[\text{HCl}]=0.8\text{ M}$ ,  $F_R=0.24\text{ ml min}^{-1}$ . Channel  $C_2$ : Water as carrier,  $V_i=243\text{ }\mu\text{l}$  of a standard solution of  $\text{BrO}_3^-$  at a concentration of  $200\text{ }\mu\text{g l}^{-1}$ ,  $F_P=0.24\text{ ml min}^{-1}$ . Channel  $C_3$ :  $[\text{NaAc}]=2.5\text{ M}$ ,  $F_A=0.24\text{ ml min}^{-1}$

thermostatted reactor was also the same because the values of  $F_R$  and  $F_P$  were constant (98 s). The time of appearance ( $t_a$ ) was the same for all cases, 120 s. The values of  $\Delta I_F$  obtained for each temperature are plotted in Fig. 5.

Upon increasing the temperature, the analytical signal increased, due to the increase in the reaction rate, such that for this reaction time a constant value of  $\Delta I_F$  was reached as from 60 °C. No conclusions could be drawn as regards the stability of the bromation product since it was not fluorescent.

From a practical point of view, it may be inferred that by thermostating the reactor at temperatures above 40 °C it is possible to accelerate the reaction rate to a sufficient extent to ensure completion of the reaction.

### Optimization of the experimental conditions

Once the kinetic characteristics of the chemical reaction were known, a study was made of each of the variables affecting the analytical signal, bearing in mind that it was necessary to differentiate between those affecting the chemical reaction and those that modified the value of the fluorescence emission intensity.

### Chemical variables

Using the flow scheme depicted in Fig. 1a, the geometric and hydrodynamic conditions were fixed at the following values:  $F_R = F_P=0.24\text{ ml min}^{-1}$ ;  $F_A=0.24\text{ ml min}^{-1}$ ,  $R=400\text{ cm}$ ;  $T=60\text{ }^\circ\text{C}$ ,  $V_i=243\text{ }\mu\text{l}$  of standard solutions of  $\text{BrO}_3^-$  at concentrations of 200 and  $600\text{ }\mu\text{g l}^{-1}$ , such that the reaction time was constant in all cases,  $t_R=110\text{ s}$ ; the contact time with the thermostatted reactor was constant,  $t_c=98\text{ s}$ , and the time of appearance was the same,  $t_a=120\text{ s}$ .

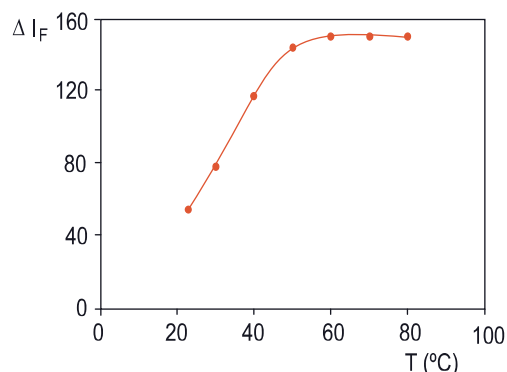


**Fig. 5** Influence of temperature on the reaction kinetics.  $C_1$ :  $[\text{CARB}]=10^{-4}\text{ M}$ ,  $[\text{KBr}]=6.7 \times 10^{-2}\text{ M}$ ,  $[\text{HCl}]=0.8\text{ M}$ ,  $F_R=0.24\text{ ml min}^{-1}$ . Channel  $C_2$ : Water as carrier,  $V_i=243\text{ }\mu\text{l}$  of a standard solution of  $\text{BrO}_3^-$  at a concentration of  $200\text{ }\mu\text{g l}^{-1}$ ,  $F_P=0.24\text{ ml min}^{-1}$ . Channel  $C_3$ :  $[\text{NaAc}]=2.5\text{ M}$ ,  $F_A=0.24\text{ ml min}^{-1}$

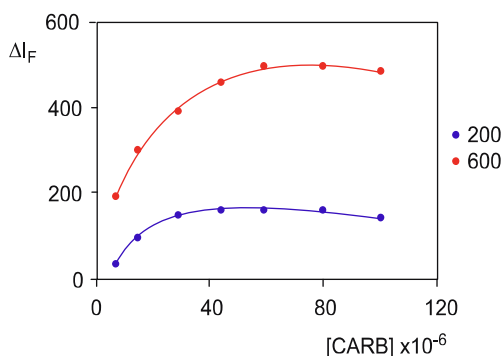


**Fig. 6** Influence of concentration of CARB. **a** 600  $\mu\text{g l}^{-1}$  of  $\text{BrO}_3^-$ , **b**: 200  $\mu\text{g l}^{-1}$  of  $\text{BrO}_3^-$ .  $[\text{KBr}] = 8.4 \times 10^{-2} \text{ M}$ ;  $[\text{NaAc}] = 2.5 \text{ M}$ .  $F_R = F_P = 0.24 \text{ ml min}^{-1}$ ;  $F_A = 0.24 \text{ ml min}^{-1}$ ;  $R = 400 \text{ cm}$ ;  $T = 60 \text{ }^\circ\text{C}$ ;  $V_i = 243 \mu\text{l}$

Except when each variable was studied, the following general conditions were imposed for the study:  $[\text{CARB}] = 10^{-4} \text{ M}$ ;  $[\text{KBr}] = 8.4 \times 10^{-2} \text{ M}$ ;  $[\text{NaAc}] = 2.5 \text{ M}$ .

**Concentration of CARB** The CARB concentration was modified between  $7.3 \times 10^{-6} \text{ M}$  and  $10^{-4} \text{ M}$ . For each concentration studied, the baseline had a different  $I_F$  value, as is logical, but what was being measured was the drop in fluorescence,  $\Delta I_F$ . The mean  $\Delta I_F$  values obtained for each concentration of the fluorescent reagent are shown in Fig. 6.

The higher the concentration of CARB, the greater the amount of bromated product formed and the higher  $\Delta I_F$ , this reaching a value after which the reaction was independent of the concentration of the fluorescent reagent. This constant value was logically different for each concentration of  $\text{BrO}_3^-$ , being  $4.0 \times 10^{-5} \text{ M}$  for 200  $\mu\text{g l}^{-1}$  and  $5.9 \times 10^{-5} \text{ M}$  for 600  $\mu\text{g l}^{-1}$ . Higher CARB concentrations led to a slight decrease in the analytical signal, probably because at those concentrations the organic molecule undergoes a process of self-absorption of the radiation emitted, the quantum yield thus decreasing.

Since the flow rates of the solutions carried by  $C_1$  and  $C_2$  were equal, the real concentrations of CARB at the point of confluence were exactly half (double dilution).

For practical purposes, it may be inferred that up to 200  $\mu\text{g l}^{-1}$  of  $\text{BrO}_3^-$  the optimum concentration at confluence for the bromation reaction is  $2.0 \times 10^{-5} \text{ M}$ , although higher concentrations up to  $5.0 \times 10^{-5} \text{ M}$  generated similar signals. The same was the case for concentrations higher than 200  $\mu\text{g l}^{-1}$  and up to 600  $\mu\text{g l}^{-1}$ ; the optimum CARB concentration was  $3.0 \times 10^{-5} \text{ M}$ , although higher ones, up to  $5.0 \times 10^{-5} \text{ M}$ , generated similar signals.

**Concentration of KBr** Once the other variables had been set at the indicated values, the concentration of  $\text{Br}^-$  in the solution flowing through channel  $C_1$  was modified from  $4.0 \times 10^{-3} \text{ M}$  to  $8.4 \times 10^{-2} \text{ M}$ , corresponding to  $2.0 \times 10^{-3} \text{ M}$  to  $4.2 \times 10^{-2} \text{ M}$  at the point of confluence where the bromation reaction begins. The results are shown in Fig. 7.

It may be seen that as the concentration of  $\text{Br}^-$  increased, so did the analytical signal, because it did this at the rate of the reaction with  $\text{BrO}_3^-$ , a constant value being reached during the reaction time studied.

For concentrations up to 200  $\mu\text{g l}^{-1}$  of  $\text{BrO}_3^-$ , the analytical signal was constant as from a  $\text{Br}^-$  concentration of  $3.0 \times 10^{-2}$  in the solution flowing through  $C_1$ , corresponding to  $1.5 \times 10^{-2} \text{ M}$  at the point of confluence, after which the chemical reaction took place. For  $\text{BrO}_3^-$  concentrations higher than 200  $\mu\text{g l}^{-1}$  (up to 600  $\mu\text{g l}^{-1}$ ), a constant analytical signal was obtained as from a slightly higher  $\text{Br}^-$  value,  $4.5 \times 10^{-2} \text{ M}$ , corresponding to  $2.25 \times 10^{-2} \text{ M}$  at the confluence point.

**HCl concentration** To study the effect of  $[\text{H}^+]$ , the concentration of HCl of the solution flowing through  $C_1$  was modified from 0.05 to 1.2 M, the rest of the variables being kept at the indicated values. The concentration of NaAc, 2.5 M, ensured that at all the HCl values studied the pH of the mixture of solutions at the second confluence point would be higher than 4.3 (a value after which the CARB species showed a constant value of fluorescence emission). For the highest HCl concentration studied, 1.22 M, the pH at the second point of confluence was 5.4.

The values of  $\Delta I_F$  obtained, as the mean value of three injections, for each  $[\text{H}^+]$  are plotted in Fig. 8.

It may be seen that the rate of the bromation reaction was independent of the concentration of  $\text{H}^+$ , a constant value of the analytical signal being reached as from  $[\text{HCl}] = 0.6 \text{ M}$ , regardless of the  $\text{BrO}_3^-$  concentration. The reaction rate increased with  $[\text{HCl}]$ , the analytical signal reaching a constant value as from 0.3 M  $[\text{HCl}]$  at the first point of confluence.

**NaAc concentration** To check the effect of the concentration of sodium acetate on the analytical signal after the chemical reaction, it was modified from 0.05 to 3.0 M. Since the concentration of HCl was kept at 0.8 M (0.4 M at

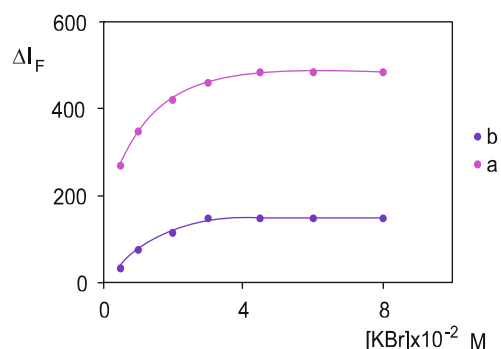


**Fig. 7** Influence of concentration of KBr. **a** 600  $\mu\text{g l}^{-1}$  of  $\text{BrO}_3^-$ , **b** 200  $\mu\text{g l}^{-1}$  of  $\text{BrO}_3^-$ .  $[\text{CARB}] = 10^{-4} \text{ M}$ ;  $[\text{NaAc}] = 2.5 \text{ M}$ .  $F_R = F_P = 0.24 \text{ ml min}^{-1}$ ;  $F_A = 0.24 \text{ ml min}^{-1}$ ;  $R = 400 \text{ cm}$ ;  $T = 60 \text{ }^\circ\text{C}$ ;  $V_i = 243 \mu\text{l}$

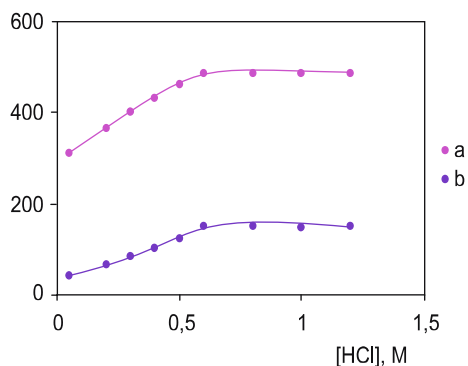


**Fig. 8** Influence of concentration of HCl. *a*  $600 \mu\text{g l}^{-1}$  of  $\text{BrO}_3^-$ , *b*  $200 \mu\text{g l}^{-1}$  of  $\text{BrO}_3^-$ .  $[\text{CARB}] = 10^{-4}$  M;  $[\text{NaAc}] = 2.5$  M.  $F_R = F_P = 0.24 \text{ ml min}^{-1}$ ;  $F_A = 0.24 \text{ ml min}^{-1}$ ;  $R = 400$  cm;  $T = 60$  °C;  $V_i = 243 \mu\text{l}$

the first point of confluence), the variations in the analytical signal obtained can only be attributed to the modification in fluorescence emission due to the variation in the concentration of the basic form of CARB. The values of  $\Delta I_F$  are plotted against the NaAc concentration in Fig. 9.

It may be observed that for values lower than 0.3 M of NaAc the analytical signal was lower than the constant value reached for higher concentrations; this is because the pH at the second point of confluence was lower than the  $\text{p}K_a + 1$ , a zone of predominance of the basic, and fluorescent, form of CARB. Bearing in mind that the concentration of HCl was diluted at the first point of confluence once a value of 0.4 M had been reached, it may be deduced that from the practical point of view the optimum ratio between  $[\text{Ac}^-]$  and  $[\text{K}^+]$  at the second point of confluence should be  $[\text{Ac}^-]/[\text{H}^+] > 0.7$ , with which the maximum value of fluorescence emission is ensured for each concentration of  $\text{BrO}_3^-$ .

#### Geometric and hydrodynamic variables

Next, a study was made of the geometric and hydrodynamic variables affecting the analytical signal for different reasons. The reaction time is governed by the flow rate from the first point of confluence; that is, the values of  $F_R$  and  $F_P$ , and the length of the reactor R. Both variables are responsible for determining the time that the reaction bolus is in the thermostatted bath, which is always slightly shorter than the reaction time. Also, the ratio between  $F_R$  and  $F_P$  controls the dilution of the reagents and, more importantly, the dilution of the sample containing  $\text{BrO}_3^-$  injected, which affects the sensitivity of the method. Finally, the value of  $F_A$  affects the rate of determination (which was not a goal of this study); more importantly, however, it also affects the dilution and hence the sensitivity of the analytical signal.

In light of the above, the study of flow rates was carried out as follows:

#### A. Influence of $F_A$ : flow rate of the sodium acetate solution

The aim of using this solution was to adjust the pH of the other mixed solutions in which the bromation reaction had occurred in order to reach a pH of  $> 4.3$  for measurement of the fluorescence of the reagent CARB. However, when at the second point of confluence of the flow scheme depicted in Fig. 1a this solution of sodium acetate was mixed with the solution in which the bromation reaction had already occurred, owing to a dilution effect the concentration of all the products generated decreased, thus affecting the sensitivity of the analytical signal.

With a view to determining the optimum value of  $F_A$  in the above flow scheme, the following conditions were fixed: Reagent solution, R:  $F_R = 0.24 \text{ ml min}^{-1}$ ,  $[\text{CARB}] = 8.0 \times 10^{-5}$ ,  $[\text{HCl}] = 1.2$  M and  $[\text{KBr}] = 8.4 \times 10^{-2}$  M. Carrier solution, P:  $F_P = 0.24 \text{ ml min}^{-1}$ ,  $V_i = 243 \mu\text{l}$  of a solution of  $\text{BrO}_3^-$  at a concentration of  $200 \mu\text{g l}^{-1}$ . Reactor 400 cm, thermostatted at 60 °C. Under these conditions, and keeping  $F_R = F_A$ , the chemical bromation reaction occurred with the optimum values of all the species involved in it.

For the sodium acetate solution, a high concentration (3.0 M) was fixed and its flow rate,  $F_A$  was modified from  $0.08 \text{ ml min}^{-1}$  to  $0.48 \text{ ml min}^{-1}$ , such that at the second point of confluence it was ensured that  $[\text{NaAc}]/[\text{H}^+] > 0.7$  in all cases, the ratio being smaller for the lowest flow rate,  $F_A = 0.08 \text{ ml min}^{-1}$ , at which the concentration ratio was 0.71.

$F_A$  flow rates lower than  $0.08 \text{ ml min}^{-1}$  (keeping  $F_R + F_A = 0.48 \text{ ml min}^{-1}$ ) elicited poor mixing at the point of confluence, leading to alterations in the diagram that affected the precision of the analytical signal. The results are shown in Fig. 10.

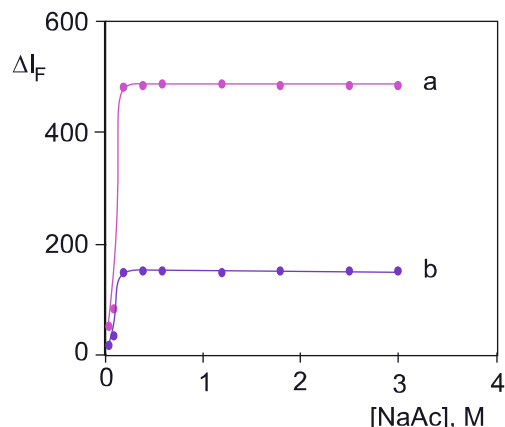


**Fig. 9** Influence of concentration of NaAc. *a*  $600 \mu\text{g l}^{-1}$  of  $\text{BrO}_3^-$ , *b*  $200 \mu\text{g l}^{-1}$  of  $\text{BrO}_3^-$ .  $[\text{CARB}] = 10^{-4}$  M.  $F_R = F_P = 0.24 \text{ ml min}^{-1}$ ;  $F_A = 0.24 \text{ ml min}^{-1}$ ;  $R = 400$  cm;  $T = 60$  °C;  $V_i = 243 \mu\text{l}$

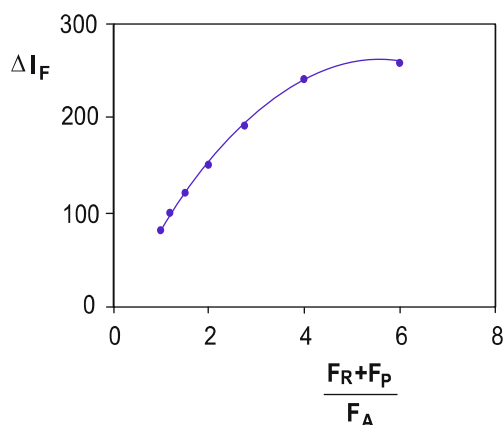


**Fig. 10** Influence of flow rate ratios between  $F_R + F_P$  and  $F_A$ . C<sub>1</sub>: [CARB]= $10^{-4}$  M, [KBr]= $8.4 \times 10^{-2}$  M, [HCl]=0.8 M,  $F_R=0.24$  ml  $\text{min}^{-1}$ . Channel C<sub>2</sub>: Water as carrier,  $V_i=243$   $\mu\text{l}$  of a standard solution of  $\text{BrO}_3^-$  at a concentration of  $200 \mu\text{g l}^{-1}$ ,  $F_P=0.24$  ml  $\text{min}^{-1}$ . Channel C<sub>3</sub>: [NaAc]=2.5 M,  $F_A=0.24$  ml  $\text{min}^{-1}$

Keeping the value of  $F_R + F_P$  constant at  $0.48 \text{ mL min}^{-1}$  in all the experiments, both the reaction time and the time of contact with the thermostatted reactor remained constant ( $t_R=98$  s,  $t_C=110$  s), such that the changes in the values of  $\Delta I_F$  can only be attributed to dilution processes of the reagent bolus upon mixing with the solution of sodium acetate. It may be seen that the lower the value of the flow rate  $F_A$  and the higher the  $F_R + F_P/F_A$  ratio, the higher the value of  $\Delta I_F$ , because the dilution of the sample injected is lower. From the point of view of analytical sensitivity it was therefore of interest to work with flow rate ratios,  $F_R + F_P/F_A$ , of the order of 6.

The increase in sensitivity was counteracted by an increase in  $\Delta t$ , the width of the diagram (FIA signal) at the baseline, as a result of the lower value of  $F_t$ , which varied between  $0.56$  and  $0.96 \text{ ml min}^{-1}$ . The value of  $t_a$  decreased in the same sense as the value of  $F_A$  increased, although its variation as from  $120$  s was difficult to measure with precision since the segment of the Teflon tube joining the second point of confluence with the flow cell was short and the times differed by less than  $2$  s.

#### B. Influence of the flow speed ratio $F_P/F_R$

The flow rates,  $F_P$  and  $F_R$ , governed the bromation reaction time as from the first point of confluence together with the time of contact between the reagent bolus and the thermostatted reactor. Additionally, at the first point of confluence the relationship between  $F_P$  and  $F_R$  affected the dilution of the standard solution or of the sample injected, and also the dilution of reagents. To study the effect of this relationship on the analytical signal, the reaction time, the contact time, the chemical variables observed in the previous study, the optimum ratio for  $F_P + F_R/F_A$ , the reaction temperature and the volumes of standard solution injected ( $243 \mu\text{l}$  of  $\text{BrO}_3^-$  at a concentration of  $200 \mu\text{g l}^{-1}$ )

were all kept constant and the values of  $F_P$ ,  $F_R$  and  $F_A$  were modified.

The value of  $F_P + F_R$  was kept at  $0.48 \text{ ml min}^{-1}$  (the optimum value deduced previously). The value of  $F_P$  was varied from  $0.22 \text{ ml min}^{-1}$  to  $0.38 \text{ ml min}^{-1}$  and at the same time  $F_R$  adopted complementary values between  $0.26$  and  $0.10$  respectively. In this range of values of  $F_P/F_R$  ( $0.85$  to  $3.8$ ) the concentration of CARB, which is the most critical reagent, was kept at the optimum value,  $2 \times 10^{-5}$ – $5 \times 10^{-5}$  M.

The flow rates were controlled with three peristaltic pumps in order to be able to modify  $F_P$ ,  $F_R$  and  $F_A$  individually at different values. The values of  $\Delta I_F$  ( $\lambda_{\text{exc}}=339$  nm,  $\lambda_{\text{em}}=430$  nm) obtained upon injecting  $243 \mu\text{l}$  of a solution of  $\text{BrO}_3^-$  at  $200 \mu\text{g l}^{-1}$  under the different experimental conditions are plotted in Fig. 11 against the  $F_P/F_R$  ratio. It may be seen that the analytical signal  $\Delta I_F$  increased with the increase in the  $F_P/F_R$  ratio because the sample injected underwent a lower dilution as the difference between the values of  $F_P$  and  $F_R$  increased.

As a practical conclusion, it may be deduced that the highest analytical signal, keeping the time constant at  $110$  s, can be obtained when  $F_P$  has a value of  $0.38 \text{ ml min}^{-1}$  and  $F_R=0.10 \text{ ml min}^{-1}$  ( $F_P/F_R=3.8$ ). It is not possible to obtain higher ratios since the CARB reagent would be diluted below the optimum values. In all the experiments the values of  $t_a$  and  $\Delta t$  were constant ( $122$  and  $180$  s respectively).

**Influence of injection volume** To study the influence of the volume of standard solution or sample injected, using the flow scheme depicted in Fig. 1b the following chemical conditions were fixed: [CARB]= $10^{-4}$  M; [HCl]= $1.2$  M, [KBr]= $8.4 \times 10^{-2}$  M, [NaAc]= $3.0$  M. The reactor length was kept at  $400$  cm, thermostatted at  $60$  °C, and in cases a standard solution of  $\text{BrO}_3^-$  at  $200 \mu\text{g l}^{-1}$  was injected. Figure 12 shows the values of  $\Delta I_F$  obtained for each experiment plotted against the volume injected.

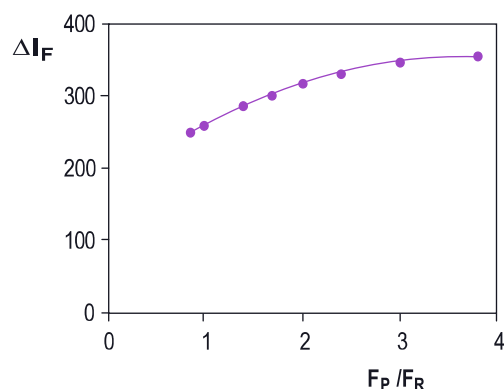


**Fig. 11** Influence of flow rate ratio,  $F_P/F_R$  keeping  $F_P + F_R=0.48$  ml  $\text{min}^{-1}$  constant and  $F_A=0.08$  ml  $\text{min}^{-1}$ . C<sub>1</sub>: [CARB]= $10^{-4}$  M, [KBr]= $8.4 \times 10^{-2}$  M, [HCl]=0.8 M. Channel C<sub>2</sub>: Water as carrier,  $V_i=243 \mu\text{l}$  of a standard solution of  $\text{BrO}_3^-$  at a concentration of  $200 \mu\text{g l}^{-1}$ . Channel C<sub>3</sub>: [NaAc]=2.5 M,  $t_R=110$  s,  $t_C=98$  s



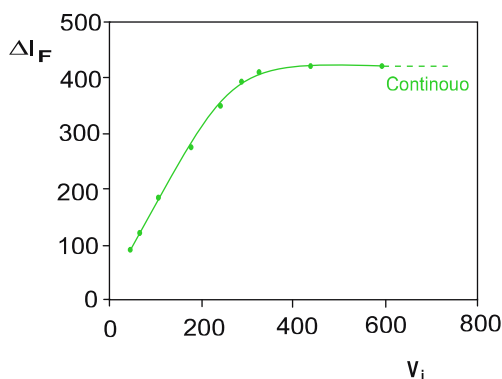


**Fig. 12** Influence of injection volume.  $C_1$ : [CARB]= $10^{-4}$  M, [KBr]= $8.4 \times 10^{-2}$  M, [HCl]=1.2 M. Channel  $C_2$ : Water as carrier, standard solution of  $\text{BrO}_3^-$  at a concentration of  $200 \mu\text{g l}^{-1}$ . Channel  $C_3$ : [NaAc]=3.0 M,  $F_R = F_A = 0.10 \text{ ml min}^{-1}$ ;  $F_P = 0.38 \text{ ml min}^{-1}$ ;  $R = 400 \text{ cm}$ ;  $T = 60^\circ \text{C}$

As expected, the larger the volume injected the higher the value of the analytical signal; this is because the dispersion of the bolus injected decreased and therefore the concentration of the analyte in that zone increased. Above 288  $\mu\text{l}$ , the increase began to be less marked, tending to reach the value obtained without dispersion because the transit of the standard solution of  $\text{BrO}_3^-$  at  $300 \mu\text{g l}^{-1}$  was in continuous mode. From the practical point of view, to conjugate sensitivity and sampling speed, which decreased with the increase in  $V_i$ , 288  $\mu\text{l}$  was chosen as a suitable injection volume. In all experiments performed,  $t_R = 110 \text{ s}$ ,  $t_c = 98 \text{ s}$ ,  $t_a = 120 \text{ s}$ .

*Influence of bromate concentration analytical calibration* Once the optimum chemical, geometric and hydrodynamic conditions had been selected, a study was made of the relationship between the concentration of  $\text{BrO}_3^-$  and the analytical signal  $\Delta I_F$ . In the flow scheme shown in Fig. 1b, the following conditions were imposed:  $C_1$ :  $F_P = 0.38 \text{ ml min}^{-1}$ ,  $V_i = 288 \mu\text{l}$ ,  $C_2$ :  $F_R = 0.10 \text{ ml min}^{-1}$ , [CARB]= $10^{-4}$  M, [HCl]=1.2 M, [KBr]= $8.4 \times 10^{-2}$  M,  $C_3$ :  $F_A = 0.10 \text{ ml min}^{-1}$ , [NaAc]=3.0 M,  $R = 400 \text{ cm}$ , thermostating temperature =  $60^\circ \text{C}$ . Standard solutions of bromate were prepared at concentrations ranging between 4 and  $200 \mu\text{g l}^{-1}$ ; these were injected into the flow system in triplicate ( $V_i = 288 \mu\text{l}$ ).

From the results obtained it was found that the values of  $\Delta I_F$  ( $\lambda_{\text{exc}} = 339 \text{ nm}$ ,  $\lambda_{\text{em}} = 430 \text{ nm}$ ) as a function of the concentration of  $\text{BrO}_3^-$  fitted a straight line with the following equation:

$$\Delta I_F = (-0.4 \pm 2.3) + (2.08 \pm 0.03) [\text{BrO}_3^-], \mu\text{g l}^{-1} R^2 = 0.9998,$$

for a level of confidence of 95%.

Under these conditions, the concentration of the limit of detection calculated by the simplified expression  $C_L = 3X_b^{\text{max}}/b$  ( $X_b^{\text{max}} = 0.6$ ) was  $0.9 \mu\text{g l}^{-1}$ . These observations indicate that method of bromate determination is clearly

more sensitive than the spectrophotometric methods described, and with a broad range of linearity, up to  $200 \mu\text{g l}^{-1}$ . This allows the measurement of  $\text{BrO}_3^-$  concentrations at around current parametric levels and those to be established in the future (recall that Japan and the USA recommend  $5 \mu\text{g l}^{-1}$ ).

*Precision of the method* To study the precision of the method, 12 standard solutions of  $\text{BrO}_3^-$  ( $n = 12$ ) containing  $5 \mu\text{g l}^{-1}$  and another 12 at concentrations higher than  $30.0 \mu\text{g l}^{-1}$  were prepared and injected ( $V_i = 288 \mu\text{l}$ ) into the flow system. After the individual values of  $\Delta I_F$  had been measured and after the corresponding statistical treatments, values of  $S_R = 3.2\%$  and  $S_R = 2.6\%$  respectively were obtained for the relative standard deviation. The determination rate was between 10 and 12 determinations per hour.

*Study of interferences*

The possible cationic and anionic interferences most frequently found in water were studied, together with other less frequent ones of interest, at varying concentrations. In this part of the work, standard solutions of  $\text{BrO}_3^-$  at  $20 \mu\text{g l}^{-1}$  with and without the interferent under scrutiny were injected under the experimental conditions found in the calibration for  $\text{BrO}_3^-$ . The results are shown in Table 1.

**Table 1** Study of interferences

Interferent	Does not interfere up to a concentration of $\leq$	Parametric value
<b>Cationic interferences</b>		
$\text{NH}_4^+$	$5 \text{ mg l}^{-1}$	$05 \text{ mg l}^{-1}$
$\text{Na}^+$	$400 \text{ mg l}^{-1}$	$200 \text{ mg l}^{-1}$
$\text{Cu}^{2+}$	$5 \text{ mg l}^{-1}$	$2 \text{ mg l}^{-1}$
$\text{Ca}^{2+}$	$400 \text{ mg l}^{-1}$	–
$\text{Mg}^{2+}$	$300 \text{ mg l}^{-1}$	–
$\text{Zn}^{2+}$	$8 \text{ mg l}^{-1}$	–
$\text{Al}^{3+}$	$350 \mu\text{g l}^{-1}$	$200 \mu\text{g l}^{-1}$
$\text{Mn}^{2+}$	$230 \mu\text{g l}^{-1}$	$50 \mu\text{g l}^{-1}$
$\text{Cd}^{2+}$	$250 \mu\text{g l}^{-1}$	$5 \mu\text{g l}^{-1}$
$\text{Fe}^{3+}$	–	–
<b>Anionic interferences</b>		
$\text{F}^-$	$2.6 \text{ mg l}^{-1}$	$1.5 \text{ mg l}^{-1}$
$\text{Cl}^-$	$350 \text{ mg l}^{-1}$	$250 \text{ mg l}^{-1}$
$\text{Br}^-$	$80 \text{ mg l}^{-1}$	–
$\text{NO}_3^-$	$100 \text{ mg l}^{-1}$	$50 \text{ mg l}^{-1}$
$\text{ClO}_3^-$	$2 \text{ mg l}^{-1}$	–
$\text{SO}_4^{2-}$	$400 \text{ mg l}^{-1}$	$250 \text{ mg l}^{-1}$
$\text{PO}_4^{3-}$	$16 \text{ mg l}^{-1}$	–
$\text{ClO}_2^-$	$5 \mu\text{g l}^{-1}$	–

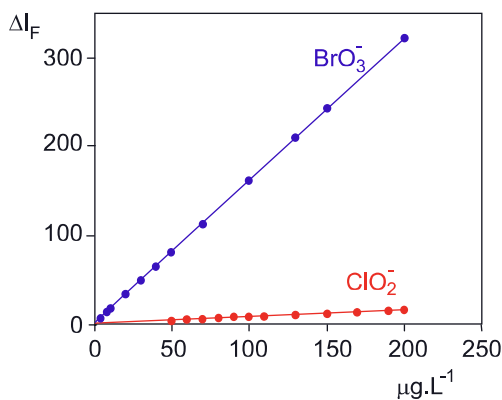


**Fig. 13** Analytical calibration for  $\text{BrO}_3^-$  at 40 °C and  $\text{ClO}_2^-$  as interferent at the same temperature.  $C_1$ : Water as carrier. Channel  $C_2$ :  $[\text{CARB}] = 10^{-4}$  M,  $[\text{KBr}] = 8.4 \times 10^{-2}$  M,  $[\text{HCl}] = 1.2$  M. Channel  $C_3$ :  $[\text{NaAc}] = 3.0$  M.  $F_P = 0.38$  ml  $\text{min}^{-1}$ ,  $F_R = F_A = 0.10$  ml  $\text{min}^{-1}$ ,  $V_i = 288$   $\mu\text{l}$ ,  $R = 400$  cm

Keeping constant the criterion of considering as an interferent any analyte that might modify the analytical signal of  $\text{BrO}_3^-$  by 5%, of all the possible interferents analyzed only  $\text{ClO}_2^-$  was found to alter the analytical signal—under the experimental condition used—by more than 5  $\mu\text{g l}^{-1}$ .

$\text{ClO}_2^-$  reacts with  $\text{Br}^-$  in acid medium, generating bromine, which then reacts with CARB, like  $\text{BrO}_3^-$ . However, in light of the analytical signals generated by both analytes for the same concentration, that of  $\text{ClO}_2^-$  being lower, it appears that in terms of speed the reaction kinetics is different.

To check this, 288  $\mu\text{l}$  of standard solutions of  $\text{ClO}_2^-$  was injected into the flow scheme shown in Fig. 1b under the experimental conditions used for the calibration for  $\text{BrO}_3^-$  at concentrations between 10 and 200  $\mu\text{g L}^{-1}$ . The values of  $\Delta\text{IF}$  obtained were plotted against the concentration of  $\text{ClO}_2^-$  and it was observed that the analytical signal,  $\Delta\text{IF}$ , fitted a straight line with an equation of:

$$\Delta I_F = (1.0 \pm 0.6) + (0.397 \pm 0.005) [\text{ClO}_2^-], \mu\text{g l}^{-1}$$

for a confidence level of 95% and a linear regression coefficient  $R^2$  of 0.999.

The slope of that line is clearly lower than that obtained under the same conditions for  $\text{BrO}_3^-$  (0.397 versus 2.08), pointing to a lower reaction rate for the case of  $\text{ClO}_2^-$ .

Regardless of the fact that the CARB bromation reaction is of analytical use for the determination of  $\text{ClO}_2^-$  in aqueous systems where there is no  $\text{BrO}_3^-$ , in order to resolve its interference in the bromate determination method the analytical measurements (signal) generated by both analytes were tested under other kinetic conditions.

The best results were obtained simple by changing the thermostating temperature of the 400-cm reactor, keeping the other variables constant at the indicated values.

The values of  $\Delta I_F$  obtained upon thermostating the reactor at 40 °C and injecting standard solutions of  $\text{BrO}_3^-$

and  $\text{ClO}_2^-$  at different concentrations are shown in Fig. 13, where—plotted against concentration—they can be seen to fit straight lines with equations of:

$$\text{BrO}_3^-: \Delta I_F = (0.2 \pm 0.2) + (1.617 \pm 0.002) [\text{BrO}_3^-], \mu\text{g l}^{-1}$$

for a confidence level of 95%.

The range of linearity for both analytical signals was kept up to 200  $\mu\text{g l}^{-1}$ , but the slope of the calibration line decreased with respect to that obtained at 60 °C.

The method for bromate determination was less sensitive at 40 °C ( $C_L = 2.2$   $\mu\text{g l}^{-1}$ ) but sufficient for application in the neighborhood of the parametric values (10–20  $\mu\text{g l}^{-1}$ ); also, at that temperature the interference by  $\text{ClO}_2^-$  decreased.

It may be concluded that  $\text{ClO}_2^-$  at 40 °C interferes in the determination of  $\text{BrO}_3^-$  in water subjected to purification when the concentration of the interferent higher than 50  $\mu\text{g l}^{-1}$ .

In order to validate the method for the determination of  $\text{BrO}_3^-$  by means of the bromation of CARB, well water (Robledo Hermoso, Salamanca, Spain) and mineral water (Aquabona) samples were spiked with standard solutions of the analyte at a final concentration ranging between 10 and 50  $\text{BrO}_3^-$  and they were determined under the calibration conditions at 60 °C.

The results obtained for both matrices are shown in Table 2; they were obtained after injecting each spiked solution in triplicate. It may be seen that for a level of confidence of 95% there is no significant difference between the  $\text{BrO}_3^-$  added and that found.

## Conclusions

This work describes a new sensitive and selective procedure for the determination of bromate that allows online measurement of trace levels of this compound in water with no need for previous separation or preconcentration steps.

The method is based on the bromation reaction of CARB in a flow system that permits kinetic control of the reaction with fluorimetric detection. The procedure, which is easy to

**Table 2** Determination of  $\text{BrO}_3^-$ , in continuous flow mode by means of the bromation reaction of carbostyryl-124

[ $\text{BrO}_3^-$ ] added ( $\mu\text{g l}^{-1}$ )	[ $\text{BrO}_3^-$ ] found ( $\mu\text{g l}^{-1}$ )	
	Well water	Mineral water
10	11±3	12±3
20	21±3	20±3
30	28±3	29±3
40	39±3	38±3
50	52±3	48±3

Validation of method

automate and simple, allows determination of the analyte across a broad concentration range (4–200  $\mu\text{g l}^{-1}$ ) with a limit of detection of 0.9  $\mu\text{g l}^{-1}$ , such that it is perfectly adaptable to the needs demanded by current legislation and those foreseen for developed countries.

## References

- Weinberg HS, Yamada H, Joice RJ (1998) New, sensitive and selective method for determining sub-mg/l levels of bromate in drinking water. *J Chromatogr A* 804:137–142
- van Staden JF, Mulaudzi LV, Stefan RI (2004) Spectrophotometric determination of bromate by sequential injection analysis. *Talanta* 64:1196–1202
- Delker D, Hatch G, Allen J, Crissman B, George M, Meter D, Kilburn S, Moore T, Nelson G, Roop B, Slade R, Swank A, Ward W, De Angelo A (2006) Molecular biomarkers of oxidative stress associated with bromate carcinogenicity. *Toxicology* 221:158–165
- Kurokawa Y, Takamura N, Matsuoka C, Imazawa T, Matsushima Y, Onodera H, Hayashi Y (1987) Comparative studies on lipid peroxidation in the kidney of rats, mice, and hamsters and on the effect of cysteine, glutathione, and diethyl maleate treatment on mortality and nephrotoxicity after administration of potassium bromate. *J Am Coll Toxicol* 6:489–501
- Kurokawa Y, Maekawa A, Takahashi M, Hayashi Y (1990) Toxicity and carcinogenicity of potassium bromate—a new renal carcinogen. *Environ Health Perspect* 87:309–335
- IARC (1986) IARC monographs on the evaluation of the carcinogenic risk of chemicals to humans. Some naturally occurring and synthetic food components, furocoumarins and ultraviolet radiation. IARC Publication No. 40, World Health Organization/IARC, Lyon, France, pp 207–220
- Crofton KM (2006) Bromate: concern for developmental neurotoxicity? *Toxicology* 221:212–216
- Council Directive 98/83/EC (1998) Official Journal of the European Communities Legislation, 1998, p 32, November 3rd
- U.S. Environmental Protection Agency, National Primary Drinking Water Regulations: Disinfectants and Disinfection Byproducts; Final Rule, Fed. Reg., 63, No. 241 (1998) 69390
- Ingrand V, Guinamant JL, Bruchet A, Brosse C, Noij ThHM, Brandt A, Sacher F, McLeod C, Elwaer AR, Croué JP, Quevauviller Ph (2002) Determination of bromate in drinking water: development of laboratory and field methods. *Trends Anal Chem* 21(1):1–12
- EPA method 300.0 (1991) EPA/600/R93/100
- EPA method 300.1 (1997) EPA/600/R98/188
- ISO/DIS (1998) 15061
- Wagner HP, Pepich BV, Hautman DP, Munich DJ (1999) Analysis of 500-ng/l levels of bromate in drinking water by direct-injection suppressed ion chromatography coupled with a single, pneumatically delivered post-column reagent. *J Chromatogr A* 850:119–129
- Wagner HP, Pepich BV, Hautman DP, Munich DJ (2000) Eliminating the chlorite interference in US Environmental Protection Agency Method 317.0 permits analysis of trace bromate levels in all drinking water matrices. *J Chromatogr A* 882:309–319
- Wagner HP, Pepich BV, Hautman DP, Munich DJ (2000) Performance evaluation of a method for the determination of bromate in drinking water by ion chromatography (EPA Method 317.0) and validation of EPA Method 324.0. *J Chromatogr A* 884:201–210
- Wagner HP, Pepich BV, Hautman DP, Munich DJ (2002) US Environmental Protection Agency Method 326.0, a new method for monitoring inorganic oxyhalides and optimization of the postcolumn derivatization for the selective determination of trace levels of bromate. *J Chromatogr A* 956:93–101
- Takayanagi T, Ishida M, Mbuna J, Driouch R, Motomizu S (2006) Determination of bromate ion in drinking water by capillary zone electrophoresis with direct photometric detection. *J Chromatogr A* 1128:298–302
- Yamanaka M, Sakai T, Kumagai H, Inoue Y (1997) Specific determination of bromate and iodate in ozonized water by ion chromatography with postcolumn derivatization and inductively-coupled plasma mass spectrometry. *J Chromatogr A* 789:259–265
- Divjack B, Novic M, Goessler W (1999) Determination of bromide, bromate and other anions with ion chromatography and an inductively coupled plasma mass spectrometer as element-specific detector. *J Chromatogr A* 862:39–47
- Dudoit A, Pergantis SA (2001) Ion chromatography in series with conductivity detection and inductively coupled plasma-mass spectrometry for the determination of nine alojen, metalloid and non-metal species in drinking water. *J Anal At Spectrom* 16:575–580
- Elwaer AR, McLeod CW, Thompson KC (2000) On-line separation and determination of bromate in drinking waters using flow injection ICP mass spectrometry. *Anal Chem* 72:5725–5730
- Valsecchi S, Isernia A, Polesello S, Cavalli S (1999) Ion chromatography determination of trace level bromate by large volume injection with conductivity and spectrophotometric detection after post column derivatisation. *J Chromatogr A* 864:263–270
- Achilli M, Romele L (1999) Ion chromatographic determination of bromate in drinking water by post-column reaction with fuchsin. *J Chromatogr A* 847:271–277
- Magnuson ML (1998) Determination of bromate at parts-per-trillion levels by gas chromatography–mass spectrometry with negative chemical ionization. *Anal Chim Acta* 377:53–60
- Silva JCGED, Dias JRM, Magalhaes JMCS (2001) Factorial analysis of a chemiluminescence system for bromate detection in water. *Anal Chim Acta* 450:175–184
- Diemer J, Heumann KG (1997) Bromide/bromate speciation by NTI-IDMS and ICP-MS coupled ion exchange chromatography. *Fresenius J Anal Chem* 357:74–79
- Creed JT, Brockhoff C (1999) Isotope dilution analysis of bromate in drinking water matrixes by ion chromatography with inductively coupled plasma mass spectrometric detection. *Anal Chem* 71:722–726
- Uraisin K, Takayanagi T, Nacapricha D, Motomizu S (2006) Novel oxidation reaction of prochlorperazine with bromate in the presence of synergistic activators and its application to trace determination by flow injection/spectrophotometric method. *Anal Chim Acta* 580:68–74